



ELSEVIER

Available online at www.sciencedirect.com

SCIENCE @ DIRECT®

Optics Communications 252 (2005) 173–178

OPTICS
COMMUNICATIONS

www.elsevier.com/locate/optcom

Second- and third-order interferometric autocorrelations based on harmonic generations from metal surfaces

Jianming Dai, H. Teng, Chunlei Guo *

The Institute of Optics, University of Rochester, 275 Hutchinson Road, Rochester, NY 14627, USA

Received 17 February 2005; received in revised form 7 April 2005; accepted 11 April 2005

Abstract

A metal-based second-order autocorrelation technique has previously been shown to be advantageous compared to conventional nonlinear crystal-based technique. In this paper, we have fully characterized the dependence of the metal-based autocorrelation signal on incident laser beam angle and light polarization. The results provide us a more complete knowledge to optimize this autocorrelation technique. Furthermore, we have extended this technique to both second- and third-order interferometric autocorrelation measurements that are more suitable for sub-20-fs ultrashort pulse measurements. These results demonstrate the potential of this autocorrelation technique for temporally characterizing ultrafast light sources with a super-broad spectrum, such as those produced from photonic-crystal fibers.

© 2005 Elsevier B.V. All rights reserved.

PACS: 42.65.Ky; 42.62.Eh

Keywords: Harmonic generation; Frequency conversion; Metrological applications

Temporal characterization of sub-picosecond laser pulses can be most conveniently achieved by using optical auto- or cross-correlation techniques [1–3]. More advanced measurements, such as those that can record both intensity and phase information, are also based on the simple correlation platform [4,5]. Traditional optical autocorrelators

typically employ the Michelson or the Mach-Zehnder interferometric geometry and use a nonlinear crystal to generate second harmonic (SHG) from two temporally overlapped pulses. Correlation functions are obtained by recording the SHG intensity as a function of the time delay between the two pulses. These correlation functions allow one to deduce the duration of short pulses, assuming a certain pulse shape. The autocorrelation technique, although straightforward, has a number of disadvantages for characterizing femtosecond

* Corresponding author. Tel.: +1 585 2752134; fax: +1 585 2444936.

E-mail address: guo@optics.rochester.edu (C. Guo).

pulses. The most significant disadvantage originates from the phase-matching requirement, which limits the spectral bandwidth that can be characterized simultaneously. For example, an ultrashort pulse with a 40-nm bandwidth will in most cases suffer some cutoff at its spectral edge simply because a nonlinear crystal only optimizes SHG over a certain wavelength range determined by the orientation of the crystal *c* axis. Even if the crystal orientation is adjusted, phase matching restricts the wavelength range over which a nonlinear crystal can be used (typically this range is restricted to at most 1000 nm) [3]. Therefore, pulses at different central wavelengths (e.g., 800 vs. 1500 nm) often require different types of crystals. In fact, no crystal is known to work efficiently for wavelengths shorter than 400 nm. Furthermore, dispersion in a nonlinear crystal itself introduces errors in ultrashort pulse measurements. Above does not account for the fact that nonlinear crystals are usually quite expensive, especially those made for special purposes (e.g., thin crystals needed for reducing dispersion).

Recently, a technique based on two-photon absorption (TPA) inside a photodetector has been developed for autocorrelation measurements [6–9]. This technique overcomes several limitations of the nonlinear crystal-based technique, as it is constrained by a much more relaxed phase-matching condition. However, it requires semiconductor materials whose bandgap energy is larger than one-photon energy but smaller than two-photon energy ($h\gamma < E_g < 2h\gamma$). Therefore, different materials are still needed for different wavelengths. This feature may restrict the suitability of such a technique when pulses have a super-broad spectrum such as those produced from photonic-crystal fibers [10,11]. Furthermore, although dispersion is greatly reduced in the TPA technique, light still needs to penetrate into the semiconductor materials over a certain depth to generate an overall output signal. As will be shown later in this paper, this dispersion still poses a less desirable effect in ultrashort pulse measurements.

More recently, we reported on an autocorrelation technique based on second harmonic generation from metal surfaces [12]. This technique not only provides excellent signal-to-noise ratio, it also

overcomes a number of disadvantages of conventional nonlinear crystal-based autocorrelation techniques. First, since SHG is generated from a few top surface layers, the phase-matching condition is therefore automatically fulfilled. Second, the measurement is virtually dispersion free since only a few atomic layers are involved, and the reflected signal is collected (avoiding material dispersion to transmitted light). Third, SHG can be generated from a metal surface over an extremely broad wavelength range. In principle, the SHG signal can be produced from far infrared to deep ultraviolet, up to the plasma frequency of the metal used (e.g., about 10 eV for gold). In our original setup, we used a non-collinear setup to avoid background signal [12]. Two incident beams are focused onto a gold sample from two opposite sides of the normal direction with the incident angle of about 65° . The generated autocorrelation SHG signal is emitted in the normal direction. The disadvantage of this setup is that the large incident angle introduces a spatial variation for the two overlapping beams and limits the accuracy when ultrashort pulses (e.g., shorter than 20 fs) are measured.

In this paper, we fully characterize the dependence of the autocorrelation SHG signal on incident laser beam angle and light polarization. The results provide us a more complete knowledge to optimize this metal-based autocorrelation technique. Furthermore, we use a collinear setup and obtain both second- and third-order interferometric autocorrelation measurements for pulses as short as 18 fs, a pulse width that is only limited by our femtosecond oscillator output.

Experimentally, a self-mode-locked Ti:sapphire oscillator running at 795 nm central wavelength with a repetition rate of ~ 94 MHz is used as our femtosecond light source. Nearly chirp-free pulses of 18 fs with a bandwidth of ~ 40 nm can be obtained with a pair of dispersive prisms for external dispersion compensation. The metal sample used here is a polycrystalline gold film. In our current setup, the two autocorrelator arms consist of two parallel beams separated by about 10 mm (Fig. 1), and this is different from our previous non-collinear setup [12]. In our experiment, the average power of each beam is about 25 mW, and these

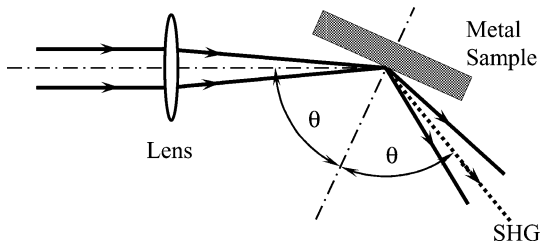


Fig. 1. Experimental setup of the near-collinear metal-based femtosecond autocorrelation technique.

two beams are focused to a same spot on the gold surface by a 125-mm focal-length lens. The two parallel beams of the autocorrelator just before the focal lens have an angle, θ , with respect to the normal direction of the sample surface. Following the focal lens, the two beams have an angle of about $\sim 5^\circ$ with respect to each other, as shown in Fig. 1. Surface SHG will be generated in the direction that bisects the angle between the two reflected fundamental beams, dictated by the energy and momentum conservation laws when one photon from each beam is absorbed simultaneously [12]. In our case, the average autocorrelation SHG power is estimated to be in the order of 1 pW [13]. The small angle between the two beams introduce a correction factor of $\cos(5^\circ/2) = 0.999$ that has a neglected effect on pulse spatial blurring. The autocorrelation function is obtained by recording the SHG signal with a photomultiplier tube (PMT) as a function of time delay between the two pulses from each arm.

Although the dependence of SHG intensity on the light polarization and incident angle have been studied in the past with a single incident beam [13–15], it is not clear that the same dependence will hold true for the autocorrelation SHG signal that results from two interacting beams. In other words, it is not clear if the autocorrelation SHG generated from two incident pulses in the direction bisecting the two reflected beams will have the same dependence on the incident angle and light polarization as the SHG generated from a single incident beam in the reflection direction. To study the polarization effect, we set the incident angle around 70° at which maximum SHG from a single incident beam was obtained [14,15]. We keep one incident beam p polarized and vary the polariza-

tion of the other beam from p to s. Autocorrelation traces are recorded at different polarization angle for one of the incident beams while keeping the other beam p polarized. The peak values of the autocorrelation traces as a function of the polarization angle of one beam is plotted in Fig. 2. The results show that, when the polarization of both beams is p, the peak autocorrelation SHG signal is maximized; the SHG signal decreases to a minimum value when the polarization of the two beams is crossed (p and s). This autocorrelation SHG signal shows the same polarization dependence as the SHG signal generated from a single beam from metal surfaces [13].

Next, we study the dependence of autocorrelation SHG signal strength on incident beam angle. The incident beam angle, θ , is the angle between the two parallel incident beams and the sample normal direction, as shown in Fig. 1. In this experiment, the polarization of both incident beams is set as p since the autocorrelation SHG signal is the highest according to the results in Fig. 2. To vary θ , the sample is carefully aligned to ensure that its rotation axis is perpendicular to the incident plane and goes through the common focal point of the two incident beams on the Au sample. Autocorrelation traces are recorded at each incident angle θ and again, the peak value of each autocorrelation trace is plotted in Fig. 3 at difference incident angle. Since the incident beam intensity on the metal sample varies with the incident angle, we further correct this effect and re-plot

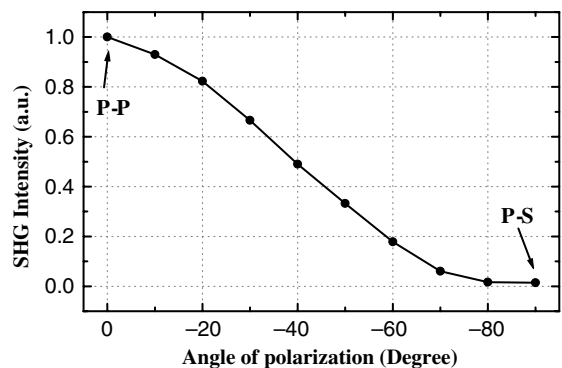


Fig. 2. Polarization dependence of the metal-based autocorrelation SHG signal.

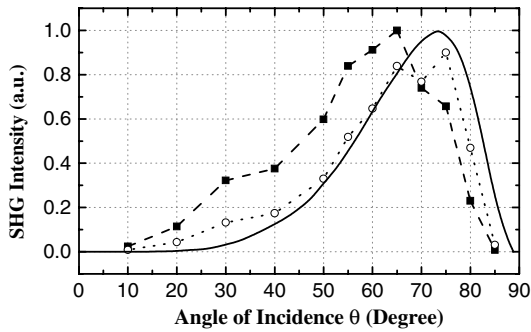


Fig. 3. Angular dependence of the metal-based SHG signal. The squared symbols are the data that do not take into account of the intensity variation at different angles; the open circle symbols are the data that take into account of the intensity variation at different angles; the solid line reproduces the model calculations from [15].

the SHG autocorrelation signal resulting from a constant incident intensity (Fig. 3). We can see that the corrected autocorrelation SHG signal shows virtually the same dependence on incident angle as the theoretical prediction based on single-beam SHG signal as well as single-beam experimental measurements [14,15]. We can see that the autocorrelation signal reaches the maximum at $\theta \sim 65^\circ$ without the intensity correction but at $\sim 70^\circ$ after the intensity correction.

To test the capability of this metal-based autocorrelation technique in characterizing ultrafast pulses, we perform second- and third-order interferometric autocorrelation measurements on ultrafast pulses from our Ti:sapphire oscillator by switching to a two-incident-beam collinear setup. The near-collinear setup discussed above has only a very small angle of $\sim 5^\circ$ between the two focusing beams (Fig. 1) and a correction factor of $\cos(5^\circ/2) = 0.999$. Thus, the optimized autocorrelation SHG condition determined above should also be a good approximation for a pure collinear setup. Therefore, for second-order interferometric autocorrelation measurement, we set the incident angle θ to be $\sim 65^\circ$ with both beams p-polarized. The second-order interferometric autocorrelation traces are obtained and plotted in Fig. 4. For comparison, second-order interferometric autocorrelation measurements on the same pulses are also obtained using the two-photon absorption technique with a GaAsP photodetector. Figs.

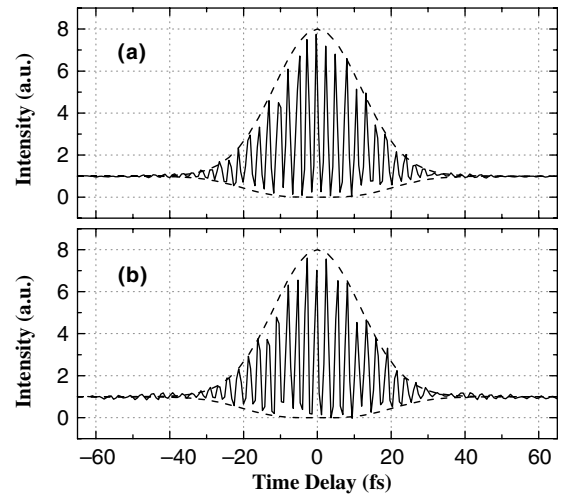


Fig. 4. Second-order interferometric autocorrelation traces (solid lines) obtained from (a) the two-photon absorption technique and (b) the metal-based surface SHG technique. The dashed lines are the envelopes of the calculated second-order interferometric autocorrelation traces of 18-fs chirp-free pulses at a central wavelength of 795 nm.

4(a) and (b) show the interferometric autocorrelation traces obtained by the TPA-based setup and metal-based setup, respectively. In the figures, the dashed lines show the envelopes of the calculated interferometric autocorrelation traces of 18-fs chirp-free pulses. As shown in the figure, the two interferometric traces are almost identical, demonstrating that the metal-based autocorrelation technique has the same capability for measuring sub-20-fs ultrashort pulses as the TPA-based technique [9].

However, if we look carefully at the two wings of each interferometric autocorrelation trace (Figs. 4(a) vs. (b)), one subtle but interesting difference can be noticed between the two traces. The interferometric autocorrelation trace obtained from our metal-based technique contains more pronounced oscillations on both wings, in the delay range of -50 to -35 fs and 35 – 50 fs. We suspect that this is an indication of some small chirp in the pulses used for the metal-based autocorrelation measurements. This is interesting because identical pulses are actually used for both metal-based and TPA-based measurements. When we examine our pulse-chirp minimization procedure

more carefully, we realize that we always start with the TPA setup to monitor the interferometric autocorrelation trace and minimize the pulse chirp and then the supposed chirp-free pulses are measured with both TPA-based and metal-based setups. However, the TPA technique relies on the two-photon absorption process inside a GaAsP photodetector, and femtosecond laser pulses need to penetrate through a focusing/protective lens in front of the GaAsP material (comes along with the detector) and also penetrate into the GaAsP material over a certain distance to generate an overall output signal through the TPA process. Thus, some small but existing dispersion should present in the TPA setup. Therefore, the chirp-minimization process using the TPA technique will leave an unavoidable negative chirp in ultrashort pulses because of this intrinsic dispersion associated with the TPA technique. When we switch to the metal-based technique to measure these same pulses, this small dispersion can be reflected in our metal-based autocorrelation traces since the metal-based setup has less intrinsic dispersion giving that surface SHG signal is generated only from a few top atomic layers in a metal. To verify our speculation, we introduce a little positive chirp into our pulses by adjusting the chirp-compensation prism pair. The oscillation signature on both wings in Fig. 4(b) can be reduced and the more identical interferometric traces can be obtained as that using the TPA autocorrelator. Therefore, we believe that our metal-based autocorrelation technique is more precise than the TPA-based technique for truly dispersion-free measurements of the duration of ultrashort optical pulses.

It is also very straightforward to perform higher-order autocorrelation measurements using our metal-based technique. It has been shown that higher-order harmonics up to fifth-order can be generated and detected from metals [16]. Experimentally, we switch our collinear experimental setup from detecting second-order autocorrelation signal to third-order one by simply replacing a 400 nm-bandpass filter by a 266 nm-bandpass filter in front of the PMT. Fig. 5 shows the third-order interferometric autocorrelation trace. The envelope of the third-order interferometric trace again agrees well with the calculation of the same 18-fs

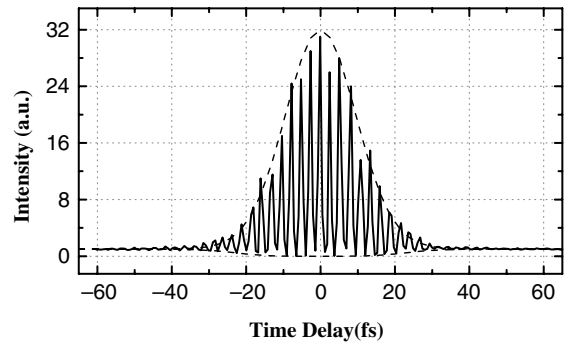


Fig. 5. Third-order interferometric autocorrelation trace (solid line) obtained from the metal-based autocorrelation technique. The dashed line is the envelop of the calculated third-order interferometric autocorrelation trace of 18-fs chirp-free pulses at a central wavelength of 795 nm.

chirp-free pulses, as for the second-order autocorrelation traces. This demonstrates that our metal-based autocorrelation technique is a reliable and convenient way for ultrashort pulse measurements. From Fig. 5, we observe a peak-to-background ratio of 32:1, and this agrees with the third-order autocorrelation calculations and experimental results obtained by Meshulach et al. [17] by using a technique based on third-harmonic generation from the surface of a glass slide.

In summary, we have fully characterized the dependence of the SHG autocorrelation signal on incident laser beam angle and light polarization. The results provide us a more complete knowledge to optimize this autocorrelation technique. In contrast to our previous non-collinear setup that introduces spatial blurring due to the large angle between the two incident beams [12], we use a collinear setup here and have obtained both second- and third-order interferometric autocorrelation traces. Pulses as short as 18 fs have been measured and the results are compared to the TPA technique. We shown that our metal-based technique has less intrinsic dispersion compared to the TPA technique. Measurements of pulses as short as 6 fs have been demonstrated with the TPA technique [9] and therefore, we expect our technique has potential capacity to measure pulses even shorter than 6 fs. This metal-based technique has significant advantages over the traditional nonlinear crystal-based autocorrelation techniques because

it is dispersion-free, provides automatic phase matching, and is capable of responding over an extremely wide spectral range. The results presented in this paper further demonstrates the potential suitability of this metal-based technique as a strongest candidate for temporally characterizing any light source with a super-broad spectrum, such as those produced from photonic-crystal fibers [10,11].

Acknowledgment

This research is supported by DARPA administered through ARO.

References

- [1] J.-C. Diels, J.J. Fontaine, L.C. McMichael, F. Simoni, *Appl. Opt.* 24 (1985) 1270.
- [2] J.-C. Diels, W. Rudolph, *Ultrashort Laser Pulse Phenomena: Fundamentals, Techniques and Applications on a Femtosecond Time Scale*, Academic Press, Boston, 1996.
- [3] E.P. Ippen, C.V. Shank, in: S.L. Shapiro (Ed.), *Ultrashort Light Pulses*, Springer, New York, 1977.
- [4] K.W. Delong, R. Trebino, *J. Opt. Soc. Am. B* 11 (1994) 2206.
- [5] C. Iaconis, I.A. Walmsley, *Opt. Lett.* 23 (1998) 792.
- [6] Y. Takagi, T. Kobayashi, K. Yoshihara, S. Imamura, *Opt. Lett.* 17 (1992) 658.
- [7] W. Rudolph, M. Sheik-Bahae, A. Bernstein, L.F. Lester, *Opt. Lett.* 22 (1997) 313.
- [8] J.K. Ranka, A.L. Gaeta, A. Baltuska, M.S. Pshenichnikov, D.A. Wiersma, *Opt. Lett.* 22 (1997) 1344.
- [9] J.K. Ranka, A.L. Gaeta, A. Baltuska, M.S. Pshenichnikov, D.A. Wiersma, *Opt. Lett.* 22 (1997) 1344.
- [10] J.K. Ranka, R.S. Windeler, A.J. Stentz, *Opt. Lett.* 25 (2000) 25.
- [11] A. Ortigosa-Blanch, J.C. Knight, P.S.J. Russell, *J. Opt. Soc. Am. B* 19 (2002) 2567.
- [12] Q. Lin, K. Wright, G.P. Agrawal, C. Guo, *Opt. Commun.* 242 (2004) 279.
- [13] S.D. Moustazis, N.A. Papadogiannis, C. Fotakis, Gy. Farkas, Cs. Tóth, *Appl. Phys. Lett.* 67 (1995) 3239.
- [14] R. Murphy, M. Yeganeh, K.J. Song, E.W. Plummer, *Phys. Rev. Lett.* 63 (1989) 318.
- [15] A.T. Georges, *Phys. Rev. A* 54 (1996) 2412.
- [16] Gy. Farkas, Cs. Tóth, *Phys. Rev. A* 46 (1992) R3605.
- [17] D. Meshulach, Y. Barad, Y. Silberberg, *J. Opt. Soc. Am. B* 14 (1997) 2122.